Design and Control of a Novel Four-degree of freedom Bearingless Permanent Magnet Machine for Flywheel Energy Storage System

Zhijia Jin[a], Xiaodong Sun[a], and Zebin Yang[b]

a Automotive Engineering Research Institute, Jiangsu University, Zhenjiang 212013, Jiangsu, China, jzjxcc@163.com, xdsun@ujs.edu.cn

b School of Electrical and Information Engineering, Jiangsu University, Zhenjiang 212013, Jiangsu, China, zbyang@ujs.edu.cn

***Abstract*—In this paper, a novel bearingless permanent magnet machine (BPMM) without strong and complex magnetic field coupling, which can limit four degrees-of-freedom (DOFs) independently, is presented for the flywheel energy storage system (FESS). The proposed machine provides suspension force by means of interaction of flux density of permanent magnet rings and winding current. And the model of the proposed machine is derived. Meanwhile, based on the conventional cross feedback control, the modified control scheme with compensation for cross channels is illustrated. Additionally, combining with the machine model and modified cross feedback controller, the simulation is built to demonstrate the effectiveness. The results show smaller fluctuation in steady state, fast response with disturbance and less impact on undisturbed channels by employing the modified control.**

I. INTRODUCTION

With the shortage of non-renewable fossil energy and stagnant development of conventional battery in the last few decades, the flywheel energy storage system (FESS) has become the research focus for many industries such as aerospace, food and pharmacy processes and electrical vehicles. FESS is a type of novel physical energy storage unit with numerous advantages, for instance, rapid charge and discharge compared to the chemical batteries. Additionally, high power capability, high reliability, low cost and long service time also make FESS an advanced application in future [1-5].

Generally, two bearingless permanent magnet machines (BPMMs) are used in the conventional FESS to supply the suspension and torque at the same time. And the 4-DOF, two translation-DOF and two rotation-DOF, are limited by controlling the suspension force generated by the two machines, simultaneously. This structure with two BPMM has been widely concerned due to its reliable operation, high efficiency and high power density. However, it also brings the shortcomings of relatively little compactness and complex magnetic field coupling. Moreover, as a complex nonlinear system, the traditional linear control schemes such as proportional-integral-differential (PID) control scheme cannot have excellent effect on the control of radial force and displacement affected by parameter variations and load disturbances [6-8]. For other bearingless motors, it is difficult, as well, to obtain a suitable linear control scheme to simplify nonlinear system control because of the existing multivariable and strong coupling, and unavoidable disturbances in bearingless motors.

If a BPMM can separate the suspension magnetic field and torque magnetic field, the strong and complex coupling would be eliminated. Then, based on the simple linear control scheme, many kinds of mature strategies can be made use of to design the appropriate controller for the novel machine. As for ordinary double magnetic bearings system, the cross feedback control is usually employed. The gyroscopic effect can be compensated through cross feedback control. And the compensation contributes to better performance and stabilizes the system. Moreover, the scheme still combines with the classic PID controller [9-12].

However, due to the uniqueness of the structure, the cross feedback control cannot satisfy every system. Furthermore, the control precision sometimes cannot meet

the requirement. Therefore, the control scheme should be modified based on different models

In this paper, a novel four-DOF BPMM for FESS is proposed. In Section II, the topology and the winding configuration of the proposed machine are described. And the principle of the suspension is explained. In Section III, the model of the machine is introduced and based on that the detailed control scheme is analyzed. In Section IV, the effect of the modified cross feedback control on the novel four-DOF BPMM is simulated. Finally, the conclusion will be drawn in Section V.

II. Topology and Principle

The topology and structure of the proposed 4-DOF BPMM is shown in Fig. 1. As shown, the machine is divided into three sections, two edging suspended sections and a central machine, respectively. The central machine is just like a common permanent magnet machine (PMM) while the stator yoke and the shaft extend outward. Meanwhile, the topology of the edging suspended section is shown in Fig. 2. The edging suspended section is made up of a disc-shaped rotor and a 12-slot stator which is similar with that of a traditional three-phase ac machine. There are two kinds of permanent magnets in the proposed BPMM, one for the central machine and the other sandwiched between the stator yoke of the edging suspended section and that of the central machine which are called as permanent magnet rings. The permanent magnet rings are magnetized axially.

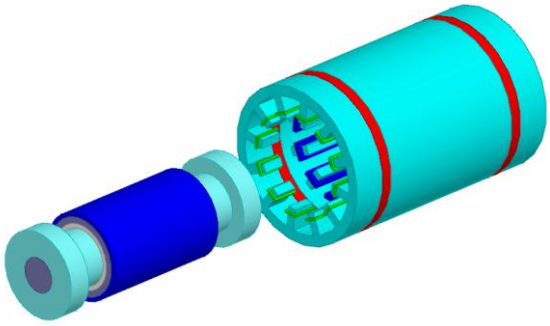

Figure 1. The structure of the proposed four-DOF machine.

Meanwhile, although the central machine and the edging suspended section have the stators with the same number of teeth, the winding distributions differ completely. As shown in Fig. 2, the suspension windings are divided into two windings, X_1 to X_6 and Y_1 to Y_6, respectively. And the central machine just utilizes the conventional three-phase windings. Besides, silicon steel sleeve is fixed outside the shaft and forms an integral unit with the disc-shaped rotors. And there is non-magnetic material sandwiched between the unit and machine permanent magnets.

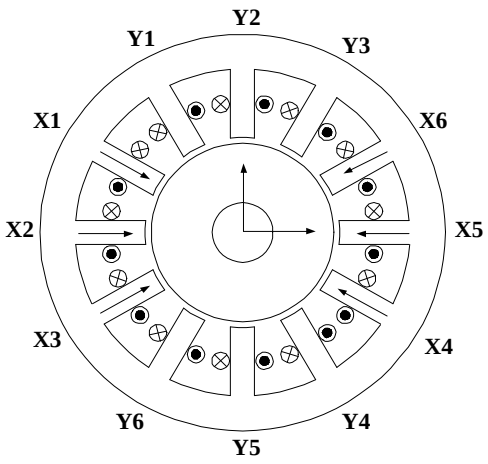

Figure 2. The winding configuration of the edging suspended section.

As for the generation of the suspension force, it can be described as the interaction of two magnetic fields. Figs. 3 and 4 show the magnetic fields generated by permanent magnet rings only and suspension current excitation only, respectively. It can be seen that the flux density generated by Y-axis suspension winding current in gap1 has the same direction with that in gap 2, while permanent magnet rings resulting the adverse flux density in the gaps in Fig. 4. Hence, the flux density increases in gap 1 and decreases in gap 2. Then, the radial suspension force towards the positive direction in the Y-axis is generated. The principle is equally applicable in the X-axis [13-14].

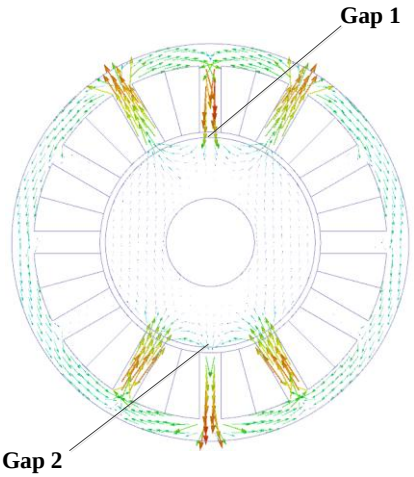

Figure 3. Flux density generated by winding current only in Y-axis.

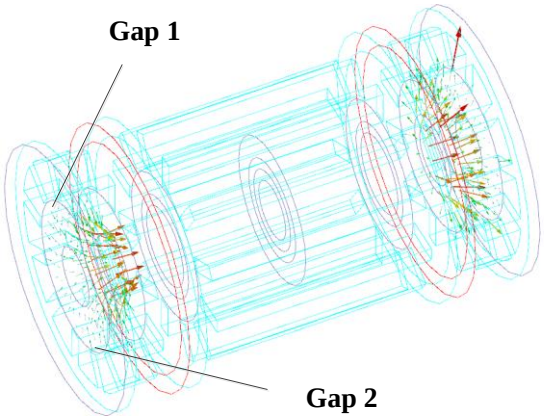

Figure 4. Flux density generated by PM only in Y-axis.

III. Control Scheme of the Machine

A. Modeling of the Machine

It can be noted that the proposed machine is suspended by two edging suspended sections. Therefore, the modeling of the machine is similar with the two 2-DOF radial magnetic bearings. A schematic of the rotor forces and the coordinate system is shown in Fig. 5, where A and B are the geometric center of the disc-shaped rotors, respectively; α, β and γ are the rotor angular displacements about the X-, Y- and Z-axis, respectively; L is the distance from the center of the central machine to the center of the disc-shaped rotor.

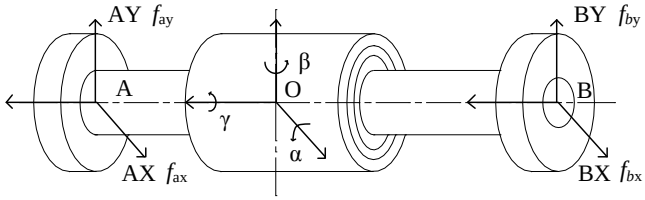

Figure 5. The schematic of the rotor forces and coordinated system.

Based on Newton's second law and principle of rotor dynamics, the model of the rotor can be described as

$$\begin{cases} m\ddot{x} = f_{ax} + f_{bx} \\ J_y\ddot{\beta} - J_z\dot{\gamma}\dot{\alpha} = L(f_{ax} - f_{bx}) \\ m\ddot{y} = f_{ay} + f_{by} \\ J_x\ddot{\alpha} - J_z\dot{\gamma}\dot{\beta} = L(f_{ay} - f_{by}) \end{cases} \tag{1}$$

where J_x, J_y and J_z are the moments of inertia of the rotor about the x-, y-, and z-axis, respectively; f_{ax}, f_{bx} , f_{ay} and f_{by} are the suspension force supported by the edging suspended section, respectively; x and y are the displacement of the mass center, respectively [15-18].

Additionally, the radial displacements can be expressed by translational and inclination displacement as written in (2).

$$\begin{cases} x_a = x_p + x_r \\ y_a = y_p + y_r \\ x_b = x_p - x_r \\ y_b = y_p - y_r \end{cases} \tag{2}$$

And the forces can also be expressed as

$$\begin{cases} F_{xp} = f_{ax} + f_{bx} \\ F_{yp} = f_{ay} + f_{by} \\ F_{xr} = f_{ax} - f_{bx} \\ F_{yr} = f_{ay} - f_{by} \end{cases} \tag{3}$$

Considering that the radial force is generated by the edging suspended sections, the equations for the translational movement expressed as

$$\begin{cases} m\ddot{x}_p = F_{xp} + 2k_x x_p \\ m\ddot{y}_p = F_{yp} + 2k_x y_p - mg \end{cases} \tag{4}$$

where k_x is the displacement-to-force coefficient. And the equations for the inclination movement are

$$\begin{cases} y = \dfrac{\dot{\gamma} Jz}{Jy} yr + \dfrac{2k_x L^2}{Jy} y_r + \dfrac{L^2}{J_y} F_{yr} \\ x = -\dfrac{\dot{\gamma} Jz}{Jx} yr + \dfrac{2k_x L^2}{Jx} y_r + \dfrac{L^2}{J_x} F_{xr} \end{cases} \tag{5}$$

Hence, Fig. 6 shows the diagram of the four-axis mechanical system where the input and output variables are the radial forces and radial displacements.

B. Cross Feedback Control

According to the four-axis model of the machine, a four-channel controller is required. Due to the similarity between the proposed model and magnetic bearings model, the cross feedback control is adopted.

The configuration of the conventional cross feedback control is shown in Fig. 7, where $G_a(s)$ is the power amplifier; G_d and G_r are transfer functions of the basic controller and the rotational cross feedback controller, respectively; i_{ax}, i_{ay}, i_{bx} and i_{by} are the control current of the edging suspended sections, respectively; x_a^*, y_a^*, x_b^* and y_b^* are the displacement references, respectively. As shown, the controller is designed for translational channels and inclination channels, respectively, owing to the gyroscopic effect.

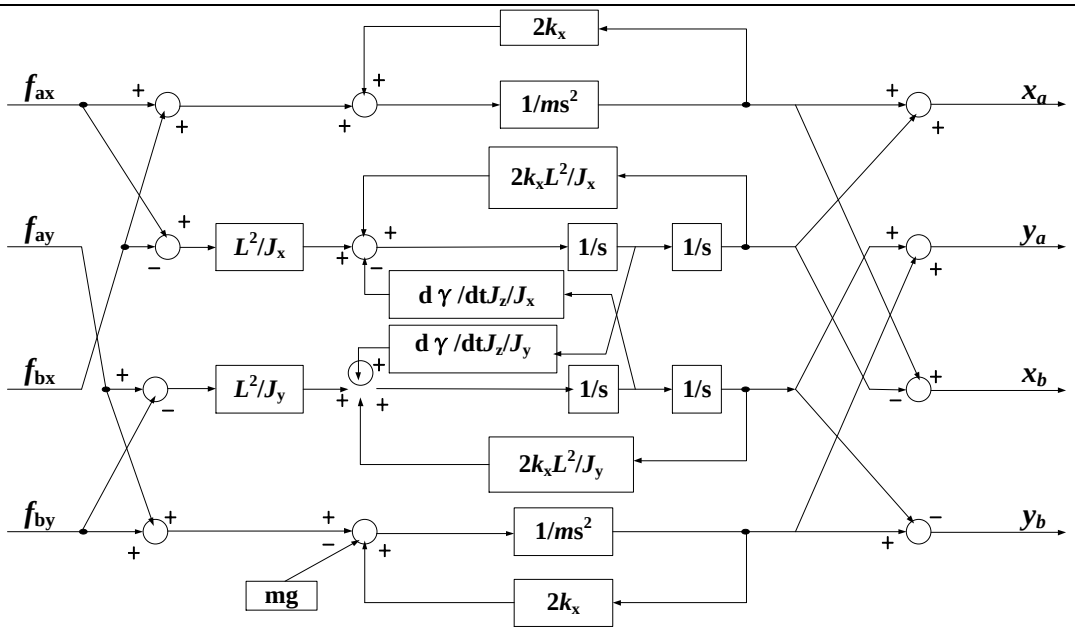

Figure 6. Diagram of the four-axis mechanical system.

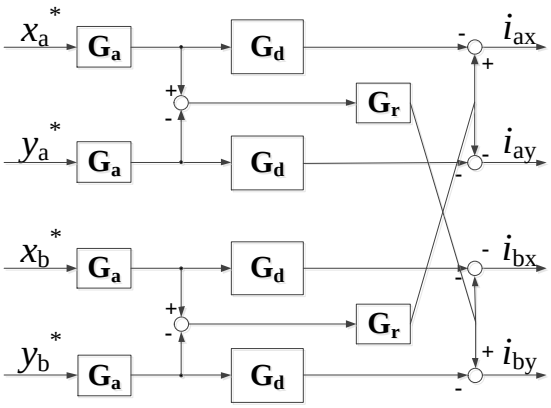

Figure 7. The configuration of the conventional cross feedback control.

However, owing to lack of the control precision, and based on the proposed machine, the conventional control scheme should be modified to achieve better effect [19-20].

C. Integral Schematic Diagram with Modified Cross Feedback Control

The integral schematic diagram is shown in Fig. 8, where Gc is the dynamic compensation filter; and G_i is the current controller; i_{ax}^*, i_{bx}^* i_{ay}^* and i_{by}^* are the current references, respectively; f_{ax}^*, f_{bx}^*, f_{ay}^* and f_{by}^* are the force displacement, respectively; k_i is the current-to-force coefficient. Compared the traditional cross feedback control, the modified controller compensates for each of two cross channels. Besides, the current controller is employed, which splits the current references into two values and outputs the difference according to the radial displacement. And then, the current-to-force coefficient k_i is multiplied to obtain the radial force references which are consider as the input of the machine model.

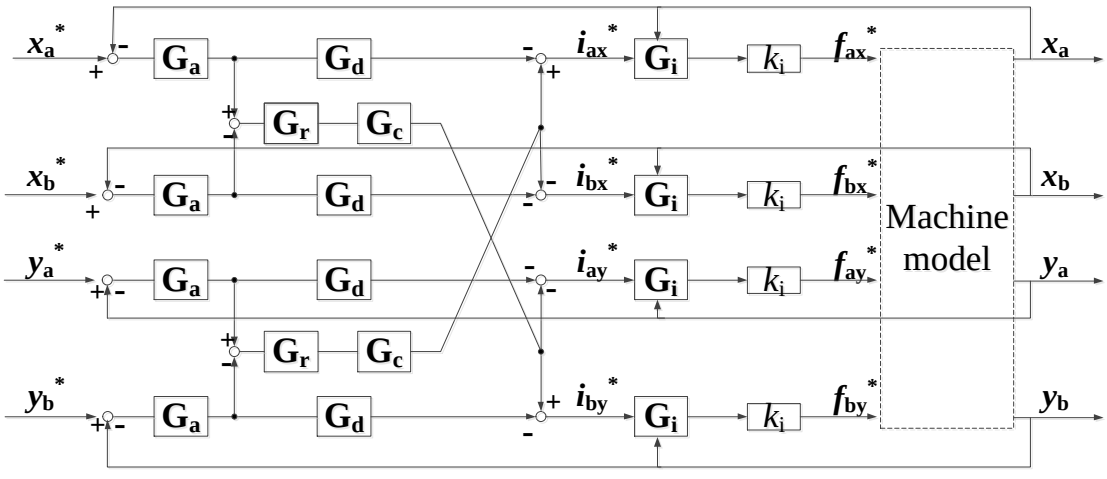

Figure 8. Integral schematic diagram with modified cross feedback control.

IV Simulation Results

In this section, the simulation has been developed to demonstrate the performance of the modified cross feedback control applied for the proposed machine.

Figs. 9 and 10 show the radial displacement responses of the proposed machine employing traditional cross feedback control and modified cross feedback control. From Figs. 9 and 10, it can be noted that the amplitude of the radial displacement with traditional scheme is about 10 μm which is a little bit larger than that with modified scheme. Meanwhile, the radial displacement responses with disturbance are also shown in Figs. 11 and 12. As for traditional cross feedback control shown in Fig. 10, after one edging suspended section receiving an interference force towards the positive direction in X-axis, the radial displacement of the section in X-axis recover to the steady status relatively slowly. And the disturbance has some certain influence on the other three channels. Contrarily, by employing the modified scheme, the radial displacement can regain stability rapidly and the influence on the other three channels reduces greatly. Therefore, it is suggested that the modified cross feedback control can realize higher control precision than that of traditional scheme.

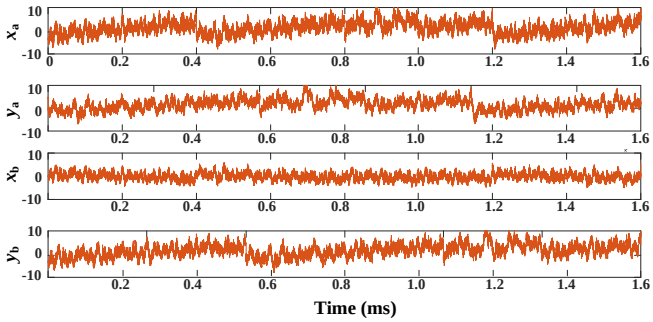

Figure 9. The displacement response based on traditional scheme.

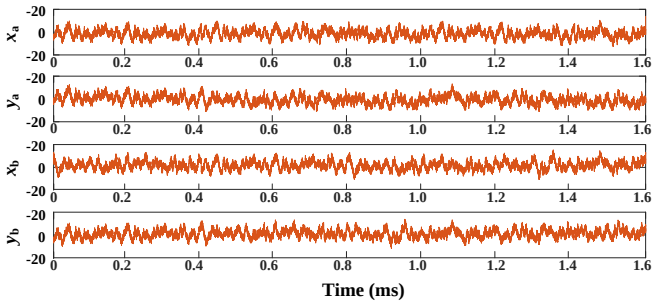

Figure 10. The displacement response based on modified scheme.

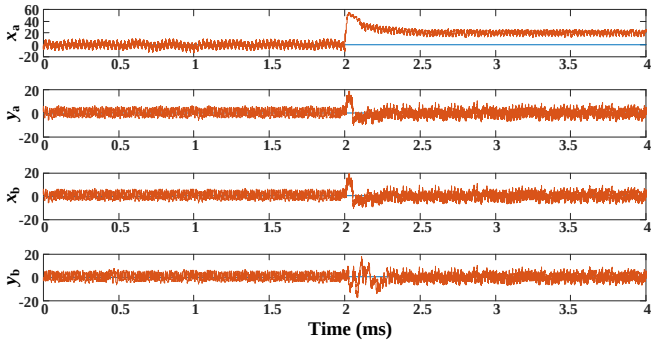

Figure 11. The displacement response with disturbance based on traditional scheme.

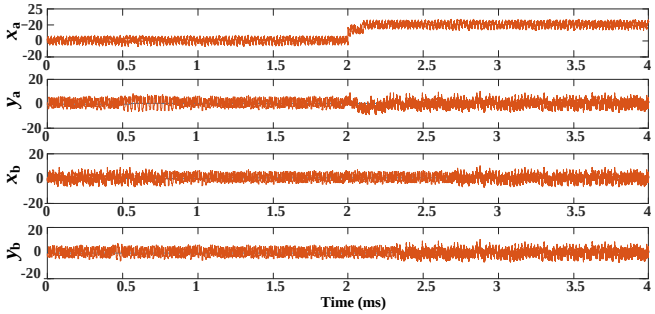

Figure 12. The displacement response with disturbance based on modified scheme

V. Conclusion

In this paper, a novel BPMM with detached suspension magnetic field and torque field is proposed. The structure of the machine, especially the edging suspended section is detailed described. Moreover, the principle of the generation of the suspension force is introduced by analyzing the flux density generated by winding current only and permanent magnet only, respectively. Additionally, based on the model of the proposed BPMM, the conventional cross feedback control has been modified with the compensation for the cross channels and current controller. Then, the simulation model has been built to demonstrate the effectiveness of the control scheme on the proposed machine. It shows that the proposed machine has fast response with sudden disturbance. A further experimental validation is undergoing.

REFERENCES

[1] X. Sun, L. Chen, and Z. B. Yang. "Overview of bearingless permanent magnet synchronous motors," *IEEE Transactions on Industrial Electronics*, vol. 60, no. 12, pp. 5528-5538, 2013.

[2] J. Fang and Y. Ren, "High-precision control for a single-gimbal magnetically suspended control moment gyro based on inverse system method," *IEEE Transaction on Industry Electronics*, vol. 58, no. 9, pp. 4331–4342, 2011.

[3] K. Zhu, Y. Xiao, and A. Rajendra, "Optimal control of the magnetic bearings for a flywheel energy storage system," *Mechatronics*, vol. 19, no. 8, pp. 1221–1235, 2009.

[4] C. Liaw, K. Hu, and J. Wang, "Development and operation control of a switched-reluctance motor driven flywheel," I*EEE Transactions on*

Power Electronics, pp. 1-1, 2018.
[5] T. Zhang, X. Liu, L. Mo, X. Ye, W. Ni, W. Ding J. Huang and X. Wang, "Modeling and analysis of hybrid permanent magnet type bearingless motor," *IEEE Transactions on Magnetics*, vol. 54, no. 3, pp. 8102-8104, 2018.
[6] Z. Tao, "Comparison and analysis of bearingless permanent magnet synchronous motor with different magnetized rotor," IEEE International Magnetics Conference, pp. 1-2, 2017.
[7] Q. Ding, T. Ni and X. Wang, "Optimal Winding Configuration of Bearingless Flux-switching Permanent Magnet Motor with Stacked Structure," *IEEE Transactions on Energy Conversion*, vol. 33 no. 1, pp. 78-86, 2018.
[8] X. Sun, Z. Xue, J. Zhu, Y. Guo, Z Yang and L Chen, "Suspension force modeling for a bearingless permanent magnet synchronous motor using maxwell stress tensor method," *IEEE Transactions on Applied. Superconductivity*, vol. 26, no. 7 pp. 1-5, 2016.
[9] H. Ouyang, F. Liu, G. Zhang and L. Mei, "Vibration suppression for rotor system of magnetic suspended wind turbines using cross-feedback-based sliding mode control," IEEE/SICE International Symposium on System Integration, pp. 112-115, 2015.
[10] M Hutterer, M Hofer and M Schrödl, "Decoupled control of an active magnetic bearing system for a high gyroscopic rotor," *IEEE Int. Conf. on Mechatronics*, pp. 210-215.
[11] S Sivrioglu and K Nonami, "LMI approach to gain scheduled H ∞, control beyond PID control for gyroscopic rotor-magnetic bearing system," *Proceedings of IEEE Conf. on Decision and Control*, 1996.
[12] I. S. Cade, P. S. Keogh and M. N. Sahinkaya, "Fault identification in rotor/magnetic bearing systems using discrete time wavelet coefficients," *IEEE/ASME Transactions on Mechatronics*, vol. 10, no. 6, pp. 648-657, 2005.
[13] T. Matsuzaki, M. Takemoto and S. Ogasawara, "Operational characteristics of an IPM-type bearingless motor with 2-pole motor windings and 4-pole suspension windings," *IEEE Transactions on Industry Applications*, vol. 53, no. 6, pp. 5383-5392, 2017.
[14] X. Sun, B. Su, L. Chen, Z. Yang, X. Xu and Z. Shi, "Precise control of a four degree-of-freedom permanent magnet biased active magnetic bearing system in a magnetically suspended direct-driven spindle using neural network inverse scheme", *Mechanical Systems and Signal Processing*, vol. 88, pp. 36-48, 2017.
[15] G. Lei, T. Wang, J Zhu, Y. Guo and S. Wang, "System level design optimization method for electrical drive systems: deterministic approach," *IEEE Transactions on Industry Electronics*, vol. 61, no. 12, pp. 6591-6602, 2014.
[16] Y Suzuki, "Acceleration feedforward control for active magnetic bearing systems excited by ground motion," *IEEE Proceedings - Control Theory and Applications*, vol. 145, no. 2, pp. 113-118, 2002.
[17] T Mizuno, M Takasaki and Y Ishino, "Controllability of gyroscopic system from a viewpoint of parallel magnetic suspension," *56th Annual Conf. of the Society of Instrument and Control Engineers of Japan*, pp. 1332-1335.
[18] X. Sun, Z. Shi, L. Chen, and Z. Yang, "Internal model control for a bearingless permanent magnet synchronous machine based on inverse system method," *IEEE Transactions on Energy Conversion*, vol. 31, no. 4, pp. 1539-1548, 2016.
[19] H. S. Zad, T. I. Khan, and I. Lazoglu, "Design and adaptive sliding mode control of hybrid magnetic bearings," *IEEE Transactions on Industrial Electronics*, vol. 65, no. 3, pp. 2537-2547, 2018
[20] M. Kandil, M. R. Dubois, L. Bakay and J. P. Trovão, "Application of second-order sliding mode concepts to active magnetic bearings," *IEEE Transactions on Industrial Electronics*, vol. 65, no. 1, pp. 855-864, 2018.